Journal of Alloys and Compounds 504S (2010) S302–S305

Contents lists available at ScienceDirect

Journal of Alloys and Compounds

journal homepage: www.elsevier.com/locate/jallcom

Decomposition of icosahedral phase in $Ti_{52}Zr_{28}Ni_{20}$ powder during electro-discharge sintering

G.A. Song[a], J.S. Shin[a], T.J. Kang[a], H.S. Choi[b], J.K. Lee[b], M.H. Lee[b], T.S. Kim[b], E. Fleury[c], F. Prima[d], W.H. Lee[a], K.B. Kim[a,*]

[a] Department of Advanced Materials Engineering, Sejong University, Gwangjin-gu, Gunja-dong, Seoul, South Korea
[b] Advanced Materials Division, Korea Institute of Industrial Technology (KITECH), Incheon, South Korea
[c] Advanced Metals Research Center, Korea Institute of Science and Technology (KIST), Seoul, South Korea
[d] Ecole Nationale Supérieure de Chimie de Paris (ENSCP), Paris, France

ARTICLE INFO

Article history:
Received 3 July 2009
Received in revised form
31 December 2009
Accepted 10 February 2010
Available online 18 February 2010

Keywords:
Quasicrystals
Powder metallurgy
Phase transitions
X-ray diffraction

ABSTRACT

A single pulse of 0.57–1.1 kJ/0.45 g-atomized spherical $Ti_{52}Zr_{28}Ni_{20}$ powders in size range of 10–30 and 30–50 μm consisting of a mixture of β-(Ti, Zr) and icosahedral phases was applied to understand the structural evolution of icosahedral phase during electro-discharge sintering (EDS). The structural analysis revealed that high electrical input energies leaded to complete decomposition of icosahedral phase into C14 Laves and β-(Ti, Zr) phases. Furthermore, the critical input energy inducing decomposition of icosahedral phase during EDS is dependent on the size of the powder.

1. Introduction

Extensive investigations on formation of quasicrystals in many alloys have been performed due to unique properties of the quasicrystals [1–4]. Among them, Ti-based icosahedral phase is considered as the second largest family of quasicrystalline alloys. Especially, the icosahedral phase in a series of Ti–Ni–Zr alloys with high degree of icosahedral perfection has received considerable attention due to their prospective applications such as the effective hydrogen storage materials [5,6].

So far, most Ti-based quasicrystalline phase has been fabricated by rapid quenching processes implying the metastability of the icosahedral phase [7]. Indeed, the characteristic of the metastable quasicrystalline phases often limits the commercial applications such as hydrogen storage materials. However, the icosahedral phase in $Ti_{53}Zr_{27}Ni_{20}$ and $Ti_{45}Zr_{38}Ni_{17}$ alloys often forms upon slow solidification exhibiting an endothermic reaction at a constant heating rate [8]. Based on the detailed analysis, it is considered that the icosahedral phase in the $Ti_{53}Zr_{27}Ni_{20}$ alloy is stable up to 650 °C [8]. On the contrary, the icosahedral phase in the $Ti_{45}Zr_{38}Ni_{17}$ alloy initially containing C14 Laves and α-Ti/Zr phases appeared up to 661 °C (i.e. slightly below the icosahedral phase transformation temperature) [8–10]. In addition, it has been reported that room-temperature high-pressure properties of the icosahedral phase in the $Ti_{53}Zr_{27}Ni_{20}$ alloy, suggesting no phase transition up to 30 GPa [11]. Therefore, the decomposition of the icosahedral phase in Ti-alloys has a strong dependence on the composition.

As mentioned above, several investigations have focused on the thermal and pressure stability of icosahedral phases. However, so far, limit investigations have been carried out to elucidate the influence of the electrical energy on the stability of icosaheral phase. In the present investigation, we focus on structural evolution of the icosahedral phase in gas-atomized $Ti_{52}Zr_{28}Ni_{20}$ powder with various electrical input energy as well as powder size during electro-discharge sintering process (EDS). Since EDS process is considered as a novel concept for both compaction and sintering of powder by applying high voltage and high current in times as short as 300 μs [12–16], it is believed that EDS is a suitable method for an assessment of a stability of icosahedral phase and mass production, which make it possible for icosahedral phase to be applicable to hydrogen storage materials. Furthermore, we have tried to understand an influence of the powder size on the decomposition of the icosahedral phase.

2. Experimental procedures

Gas-atomized spherical $Ti_{52}Zr_{28}Ni_{20}$ powders in two size ranges (10–30 and 30–50 μm) were weighed by 0.45 g, and then vibration was used to fill the powders into a quartz tube with a diameter of 4.0 mm that had a copper electrode at the

* Corresponding author. Tel.: +82 2 3408 3690; fax: +82 2 3408 3664.
E-mail address: kbkim@sejong.ac.kr (K.B. Kim).

0925-8388/$ – see front matter © 2010 Elsevier B.V. All rights reserved.
doi:10.1016/j.jallcom.2010.02.060

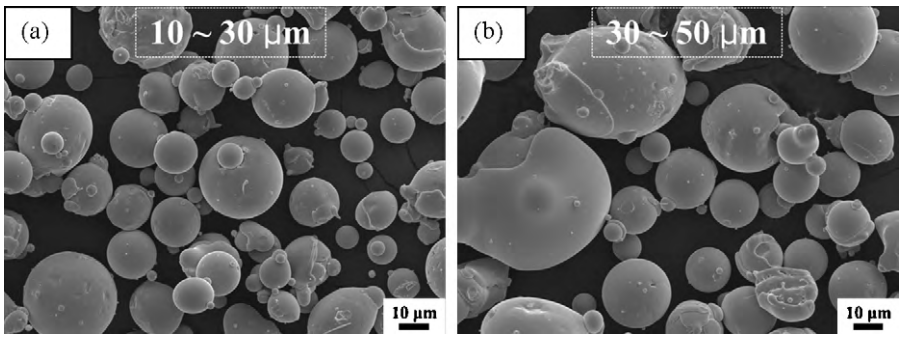

Fig. 1. SEM images of the $Ti_{52}Zr_{28}Ni_{20}$ powders fabricated by using gas-atomization ((a) 10–30 μm and (b) 30–50 μm).

bottom. Another copper electrode was placed into the upper quartz tube. The prepared green compact collective was set into the discharging chamber followed by evacuation of 2×10^{-3} Torr. The input energy can be predetermined by controlling input voltage (V) according to the equation:

$$E = \frac{CV^2}{2} \quad (1)$$

where C is the capacitance of a capacitor [17].

One capacitor bank (450 μF) was charged with four different electrical input energies (0.57, 0.7, 0.9 and 1.1 kJ). The four different input energies were imposed into the prepared green compact collectives by on/off high vacuum switch which closes the discharge circuit. When the circuit was closed, the voltage and the current take place in the powder column. The overall process is referred to as electro-discharge sintering (EDS). More detailed EDS process is described elsewhere [14].

The phase identification for the gas-atomized $Ti_{52}Zr_{28}Ni_{20}$ powders and the discharged compacts was done in D/MAX-2500/PC X-ray diffractometer (XRD) using Cu Kα radiation. A differential scanning calorimeter (DSC) was used to analyze the thermal stability of the $Ti_{52}Zr_{28}Ni_{20}$ powders against phase transformation under a flowing pure argon atmosphere at a heating rate of 20 K/min. The gas-atomized $Ti_{52}Zr_{28}Ni_{20}$ powder was examined using scanning microscopy (SEM) to observe the powder morphology and measure the powder size. Transmission electron microscopy (TEM: JEM 2010) was used to analyze a structural characterization of selected discharged compact (10–30 μm, 2.2 kV). Thin foils for TEM were prepared by a conventional ion milling (Gatan, Model 600).

3. Results and discussion

Fig. 1 shows SEM micrographs of as-prepared $Ti_{52}Zr_{28}Ni_{20}$ powders fabricated by gas-atomization under different conditions to yield two particle size classes. The size of the $Ti_{52}Zr_{28}Ni_{20}$ powder in Fig. 1(a) can be measured to be 10–30 μm whereas that in Fig. 1(b) to be 30–50 μm. The morphology of $Ti_{52}Zr_{28}Ni_{20}$ powders with different size range is quite spherical indicating the gas-atomization process is effective to produce spherical powders.

In order to conform formation of icosahedral phase in the $Ti_{52}Zr_{28}Ni_{20}$ powders with different size range, X-ray diffraction (XRD) and differential scanning calorimeter (DSC) analysis were carried out. Fig. 2(a) shows XRD diffraction traces of the $Ti_{52}Zr_{28}Ni_{20}$ powders with the different size range, i.e. 10–30 and 30–50 μm, respectively. The main sharp diffraction peaks of the $Ti_{52}Zr_{28}Ni_{20}$ powders in Fig. 2(a) are more or less identical, indicating there is no significant change on the phase formation. Furthermore, the diffraction maxima can be identified as a mixture of solid solution β-(Ti, Zr) and icosahedral phases. It has been reported that Ti–Zr–Ni alloys produced by melt spinning with Ti concentrations around 50 at.%, i.e. $Ti_{53}Zr_{27}Ni_{20}$, consist of fully icosahedral phase [8]. In the present study, the $Ti_{52}Zr_{28}Ni_{20}$ powders are composed of small amount of the β-(Ti, Zr) phase besides icosahedral phase. However, the relative diffraction intensity of the icosahedral phase is considerably higher than that of the β-(Ti, Zr) phase, indicating high volume fraction of the icosahedral phase. The DSC traces recorded upon a constant-rate heating at 20 K/min are shown in Fig. 2(b). Both $Ti_{52}Zr_{28}Ni_{20}$ powders with the difference in size exhibit single exothermic peak around 566–636 °C. In general, the icosahedral phase in Ti–Ni–Zr alloys with Ti concentrations around 50 at.% is stable up to 650 °C, exhibiting endothermic reaction during DSC with high vacuum atmosphere [8]. However, the present DSC result displays single exothermic reaction around 566–636 °C. This argument is possibly due to the influence of the oxygen content on the phase stability of the icosahedral phase [8]. The enthalpies of the exothermic reaction are 64.42 J/g for 10–30 μm and 27.57 J/g for 30–50 μm, respectively. This enthalpy difference is believed to result from the amount of icosahedral phase existing in the powder, suggesting that the $Ti_{52}Zr_{28}Ni_{20}$ powder with size range of 10–30 μm contains higher amount of icosaheral phase rather than the $Ti_{52}Zr_{28}Ni_{20}$ powder with size range of 30–50 μm.

Four different input electrical energies (0.57, 0.7, 0.9 and 1.1 kJ) were imposed into the $Ti_{52}Zr_{28}Ni_{20}$ powders comprising solid solution β-(Ti, Zr) and icosahedral phases to observe structural evolution. Each experimental condition and constitutive phase in the powder and the compacts are listed in Table 1. Fig. 3 shows XRD traces of the $Ti_{52}Zr_{28}Ni_{20}$ compacts produced by various EDS conditions. The main sharp diffraction peaks of the $Ti_{52}Zr_{28}Ni_{20}$ compacts produced using $Ti_{52}Zr_{28}Ni_{20}$ powder in size range of 10–30 μm under input energy of 0.57 kJ in Fig. 3(a) is identified as a mixture of C14 Laves and icosahedral phases, implying that applied input energy (0.57 kJ) was not sufficient to lead the decomposition of the icosahedral phase. With further increase in input energy from 0.7 to 1.1 kJ icosahedral phase is completely transformed into β-(Ti, Zr) and C14 Laves phases, as similar to the thermal phase transformation [8]. Similarly, the icosahedral phase is entirely transformed into β-(Ti, Zr) and C14 Laves phases in the $Ti_{52}Zr_{28}Ni_{20}$ compacts discharged under high input energy (0.9 and 1.1 kJ) as shown in Fig. 3(b). However, the icosahedral phase still exists in the $Ti_{52}Zr_{28}Ni_{20}$ compacts discharged under 0.7 kJ in Fig. 3(b) compared to the $Ti_{52}Zr_{28}Ni_{20}$ compacts discharged under 0.7 kJ shown in Fig. 3(a), implying that generation of the energy, i.e. joules heat in the powder column during EDS, is strongly dependent on the powder size. The green compact composed of small powders has the higher specific surface area compared to that composed of large powders. It is plausible to regard the surface of the powder as a heat source. Therefore, it is expected that the powder size has a strong influence to control the stability of the icosahedral phase during EDS.

Table 1
Experimental condition and constitutive phase of the $Ti_{52}Zr_{28}Ni_{20}$ compacts fabricated by EDS under each condition.

Capacitance (μF)	Voltage (kV)	Input energy (kJ)	Constitutive phase	
			10–30 μm	30–50 μm
–	–	–	i-phase β-(Ti, Zr)	i-phase β-(Ti, Zr)
450	1.6	0.57	i-phase C14 Laves	i-phase C14 Laves
450	1.8	0.7	β-(Ti, Zr) C14 Laves	i-phase C14 Laves
450	2.0	0.9	β-(Ti, Zr) C14 Laves	β-(Ti, Zr) C14 Laves
450	2.2	1.1	β-(Ti, Zr) C14 Laves	β-(Ti, Zr) C14 Laves

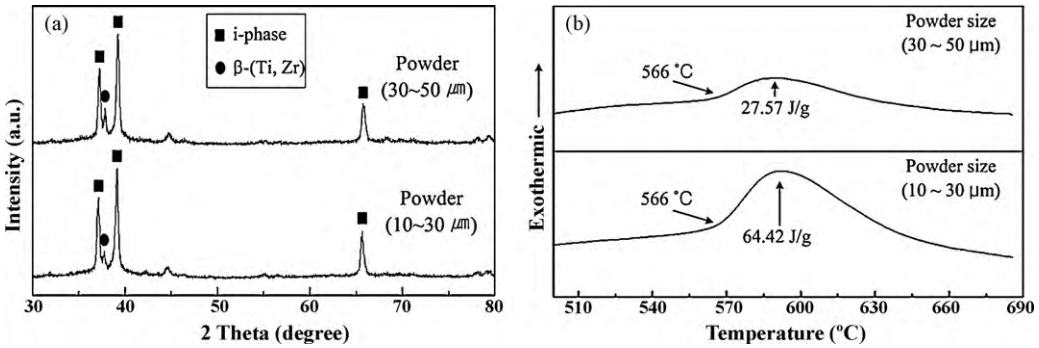

Fig. 2. XRD (a) and DSC (b) traces of the $Ti_{52}Zr_{28}Ni_{20}$ powders with size range in 10–30 and 30–50 μm.

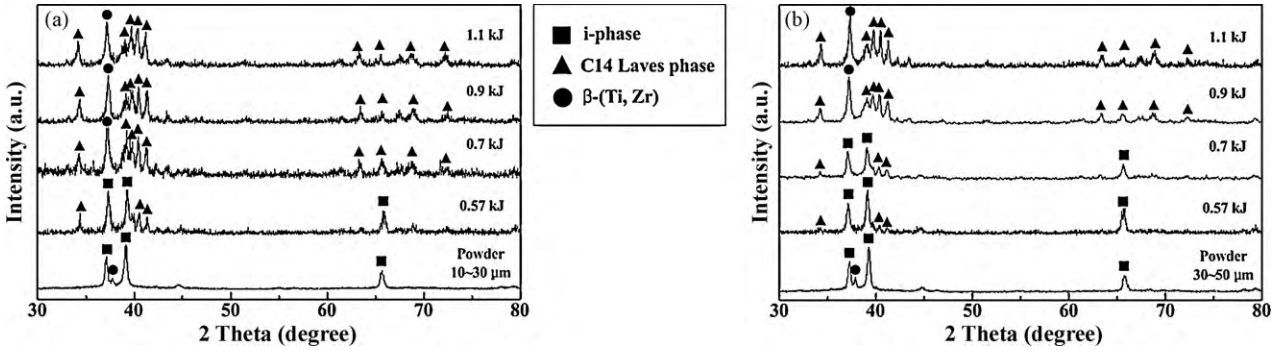

Fig. 3. XRD traces of the $Ti_{52}Zr_{28}Ni_{20}$ compacts produced using the $Ti_{52}Zr_{28}Ni_{20}$ powders with size range in 10–30 μm (left) and 30–50 μm (right) by EDS under different conditions (0.57, 0.7, 0.9 and 1.1 kJ) well as the $Ti_{52}Zr_{28}Ni_{20}$ powders.

Fig. 4 shows TEM bright field image and selected area diffraction patterns (SADPs) of the $Ti_{52}Zr_{28}Ni_{20}$ compacts discharged using powder in size range of 10–30 μm under input energy of 1.1 kJ. Fig. 4(a) displays that fine lamellae with dark contrast and 15 nm in width as denoted by 'b' is homogeneously embedded in the matrix with gray contrast as indicated by 'c'. The SADP in Fig. 4(b) obtained from the region 'b' in Fig. 4(a) corresponds to the [1 1 0] zone axis of the C14 Laves phase. The SADP in Fig. 4(c) obtained from the region 'c' in Fig. 4(a) is identified as the [1 0 0] zone axis of the β-(Ti, Zr) solid solution phase. This phase analysis through TEM is in good agreement with XRD in Fig. 2, strongly supporting that complete phase transformation form icosahedral phase to β-(Ti, Zr) and C14 Laves phase occurs by the electrical input energy.

Based on the XRD and DSC analyses, the phase transformation of icosaheral phase in the $Ti_{52}Zr_{28}Ni_{20}$ powder depends on the applied energies. Moreover, the critical input energy causing the decomposition of the icosahedral phase depends on the powder size in Fig. 3. That indicates that the icosaheral phase of the $Ti_{52}Zr_{28}Ni_{20}$ powder in size range of 10–30 μm is accelerated to transformation of the icosahedral phase into C14 Laves and β-(Ti, Zr) phases during EDS at low input energy (0.7 kJ). This implies that the powder size plays a crucial role to control the induced-electrical energy, i.e. Joule's heat during EDS. It is plausible to regard the surface of the powder as a heat source. Therefore, it is expected that the increase of the powder size can be effective to decrease the induced-electrical energy and

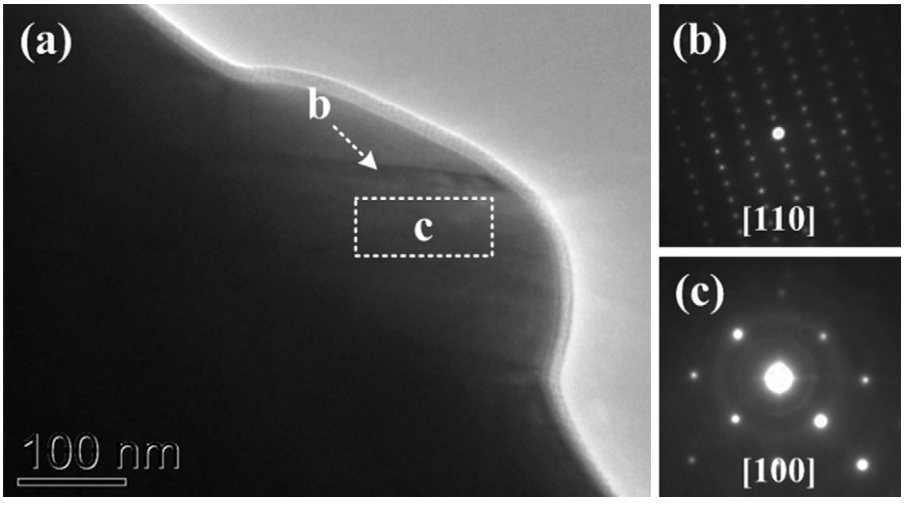

Fig. 4. TEM bright field image (a) and selected area diffraction patterns [(b) and (c)] of the $Ti_{52}Zr_{28}Ni_{20}$ compacts discharged using powder in size range of 10–30 μm under input energy of 1.1 kJ; (b) [1 1 0] zone axis of the C14 Laves phase; (c) [1 0 0] zone axis of the β-(Ti, Zr) phase.

thus retarding the decomposition of the icosahedral phase during EDS.

4. Summary

Electro-discharge sintering (EDS) was used to observe structural evolution of gas-atomized $Ti_{52}Zr_{28}Ni_{20}$ powder with a different size range (10–30 and 30–50 μm) consisting of a mixture of β-(Ti, Zr) and icosahedral phases. Different electrical input energies (0.57–1.1 kJ) with a constant capacitance of 450 μF was imposed into the powder column with a diameter of 4.0 mm. Icosahedral phase still existed in the compact even after EDS upon low input energy for both powders. However, the icosahedral phase in the powders is completely decomposed into C14 Laves and β-(Ti, Zr) phases with increasing the input electrical energy. In addition, the decomposition of the icosahedral phase in the powder with a size range of 10–30 μm is accelerated even at low input energy (0.7 kJ) compared to that in the powder with a size range of 30–50 μm, supporting that the increase of the powder size suppresses the decomposition of the icosahedral phase even under high input energy during EDS.

Acknowledgements

This work was supported by Korea Science & Engineering Foundation through the Joint Research Program (Grant No. F01-2008-000-10048-0) and a grant from the Fundamental R&D Program for Core Technology of Materials funded by the Ministry of Knowledge Economy, Republic of Korea.

References

[1] C. Janot, R. Mosseri (Eds.), Proceedings of the 5th International Conference on Quasicrystals, 1995, World Scientific, Singapore, 1995.
[2] S. Takeuchi, T. Fujiwara (Eds.), Proceedings of the 6th International Conference on Quasicrystals, 1997, World Scientific, Singapore, 1998.
[3] D.H. Bae, S.H. Kim, D.H. Kim, W.T. Kim, Acta Mater. 50 (2002) 2343.
[4] D.H. Bae, M.H. Lee, K.T. Kim, W.T. Kim, D.H. Kim, J. Alloys Compd. 342 (2002) 445.
[5] K.F. Kelton, P.C. Gibbons, MRS Bull. 22 (1997) 69.
[6] A.M. Viano, R.M. Stroud, P.C. Gibbons, A.F. McDowell, M.S. Conradi, K.F. Kelton, Phys. Rev. B 51 (1995) 12026.
[7] K.F. Kelton, in: J.H. Westbrooke, R.L. Fleischer (Eds.), Intermetallic Compounds: Principles and Practice, Wiley, New York, 1995, p. 453.
[8] R.M. Stroud, K.F. Kelton, S.T. Misture, J. Mater. Res. 12 (1997) 434.
[9] K.F. Kelton, W.J. Kim, R.M. Stroud, Appl. Phys. Lett. 70 (1997) 3230.
[10] R.M. Stroud, A.M. Viano, P.C. Gibbons, K.F. Kelton, S.T. Misture, Appl. Phys. Lett. 69 (1996) 2998.
[11] R. Nicula, A. Jianu, U. Ponkratz, E. Burkel, Phys. Rev. B 62 (2000) 8844.
[12] W.H. Lee, C.Y. Hyun, J. Mater. Process. Technol. 189 (2007) 219.
[13] Y.B. An, W.H. Lee, Mater. Chem. Phys. 95 (2006) 242.
[14] Y.J. Jo, C.M. Lee, H.S. Jang, N.S. Lee, J.H. Suk, W.H. Lee, J. Mater. Process. Technol. 194 (2007) 121.
[15] Y.J. Cho, C.M. Lee, H.S. Chang, N.S. Lee, K.B. Kim, E.C. Jeon, J.H. Sok, H. Kwon, K.B. Lee, W.H. Lee, Scr. Mater. 57 (2007) 129.
[16] Y.B. An, N.H. Oh, Y.W. Chun, Y.H. Kim, J.S. Park, K.O. Choi, T.G. Eom, T.H. Byun, J.Y. Kim, C.Y. Hyun, D.K. Kim, C.S. Byun, J.H. Sok, J.J. Kwon, W.H. Lee, Scr. Mater. 53 (2005) 905.
[17] Y.W. Cheon, Y.J. Jo, C.M. Lee, H.S. Jang, K.B. Kim, W.H. Lee, Mater. Sci. Eng. A 467 (2007) 89.